

Au-Ag nanoparticles-graphene quantum dots as sensor for highly sensitive electrochemical determination of insulin level in pharmaceutical samples

Jing Wang*, Chunyan Liu, Juan Hua

Yantai Qishan Hospital, Yantai, 264001, China

*E-mail: ycwj007@163.com

Received: 26 May 2021/ Accepted: 13 July 2021 / Published: 10 September 2021

This study was performed on the synthesis of Au-Ag nanoparticles-graphene quantum dots (Au-Ag NPs/GQDs) as a highly sensitive electrochemical sensor of insulin levels in prescription drugs for type 2 diabetic patients. To fabricate the Au-Ag NPs/GQDs modified GCE electrode (Au-Ag NPs/GQDs/GCE), GQDs were synthesized using the hydrothermal method on GCE, and then Au-AgNPs were electrodeposited on GQDs/GCE. The structural analyses of Au-Ag NPs/GQDs/GCE using SEM and XRD showed uniform coverage of the bimetallic nanoparticles in fcc crystal structure on the GQDs. The electrochemical studies for determination of insulin using CV and DPV showed that the linear range, limit of detection and sensitivity were obtained 10 to 120 μM , 1.1 nM and 0.24184 $\mu\text{A}/\mu\text{M}$, respectively which were comparable or better than sensing results of other reported insulin sensors in literature. The selectivity of proposed insulin sensor was investigated in presence of biological species human serum sample such as thiourea, glucose, methionine, cysteine, ascorbic acid, uric acid and glutathione and results indicated the interference biological species did not show any interference effect on insulin determination. The applicability of sensor was studied for the determination of insulin in insulin glargine injection sample and results exhibited to the acceptable values for recovery and RSD, demonstrating the proposed sensor can be used as reliable and precise sensor to determine insulin in biological and clinical samples.

Keywords: Insulin; Differential pulse voltammetry; Au-Ag Nanoparticles; Graphene quantum dots; Electrodeposition

1. INTRODUCTION

Diabetes as a group of metabolic disorders refers to high blood sugar (glucose) level over a prolonged period of time [1, 2]. Diabetes occurs either when the pancreas does not produce enough insulin and when the body cannot effectively use the insulin it produces which are known as type 1 diabetes, and type 2 diabetes, respectively [3, 4]. Symptoms often include excessive excretion of urine, constant hunger, increased thirst, weight loss, nausea and vomiting, stomach pain, weakness or fatigue,

shortness of breath, fruity-scented breath and confusion [5-7]. An untreated diabetic can lead to many health complications such as diabetic ketoacidosis, hyperosmolar hyperglycemic state, cardiovascular disease, stroke, chronic kidney disease, foot ulcers, damage to the nerves, and damage to the eyes, cognitive impairment, and death [8, 9]. Therefore, determining the insulin level in blood, urine, and medicine is important [10, 11].

Many studies have been performed to detection insulin using clamp technique, micellar electrokinetic capillary chromatography, liquid chromatography, mass spectrometry, high-performance liquid chromatography, immunofluorometry and electrochemical methods [12-14]. Studies have been continued to developing the selective insulin sensors in biological media for the elimination of interference effect of species [15-17]. Another important property of insulin sensors is a low detection limit because the normal level of insulin in the blood is 111-1917pM [18, 19]. Meanwhile, many of these techniques are expensive and time-consuming, and have been shown to lack of selectivity in biological and pharmaceutical environments. Among the analytical methods of insulin, electrochemical techniques as interesting and low-cost techniques can improve the sensing properties through modification the electrode surfaces with composites, hybrids, and nanostructured materials [20-22]. Therefore, this study was conducted on the synthesis of Au-Ag nanoparticles-graphene quantum dots as a fast, low cost and highly sensitive electrochemical sensor of insulin level in Lantus as long-acting insulin and prescription drug which approved to treat children and adults with type 2 diabetes.

2. MATERIALS and METHOD

Before modification GCE, the GCE surface was cleaned using polishing on alumina slurry (0.3, and. 0.05 μm , 99.99%, Sigma-Aldrich) in sequence to reach the mirror surface, and rinsed with distilled water and ethanol, respectively. In order synthesis of GQDs using hydrothermal method [23], 10 mL of 0.2 M citric acid (99%, Shandong Bohua Chemical Co., Ltd., China) solution was transferred to 25 ml hydrothermal synthesis autoclave reactor with Teflon lined vessel at 175°C for 9 hours. Next, the flask of the obtained brownish solution was placed on rotary evaporator and concentrated. Then, the concentrated GQDs suspension was dried in air. Then, 5mg of GQDs were ultrasonically added into 2 mL phosphate buffer solution (PBS) pH 7 to achieve a homogeneous suspension of GQDs. For modification the GCE by GQDs [24], the electrodeposition was applied on an electrochemical work station (PGSTAT30, Metrohm, Autolab B.V., Utrecht, The Netherlands) in a three electrode system (GCE as working electrode, platinum wire as an auxiliary electrode and Ag/AgCl (3M KCl) as reference electrode) through cyclic voltammetry (CV) technique in the prepared homogeneous suspension of GQDs as electrolyte under the potential range between 0 and 1.0 V at a scan rate of 20 mV/s for seventy cycles.

For modification of the GQDs/GCE by Au-Ag NPs [25], an aqueous solution of the mixture of 5 mL of 0.5 mM NaAuCl₄ (99%, Merck, Germany), 5 mL of 0.5 mM AgNO₃ ($\geq 99.0\%$, Merck, Germany), 2 mL of mixture of 10 mM Na₂SO₄ (99%, HongzhiXimi (Guangdong) New Material Co., Ltd., China) and 2mL of 0.1 mM H₂SO₄ (96%, Sigma-Aldrich) prepared as electrodeposition

electrolyte of Au-Ag nanoparticles. The electrochemical deposition was performed under the potential range between -1.5 to 2.0 V and at a scan rate of 20mV/s for seventy cycles.

For preparation of the real sample, Lantus (insulin glargine injection) was provided from a local pharmacy which labelled each milliliter of Lantus contains 100 IU (3.6378 mg) insulin glargine (0.6344 mM). It was added to 0.1 M PBS pH 7 in equal ratio. The standard addition method was used for analytical analysis of the prepared real sample.

Electrochemical studies were conducted using CV and differential pulse voltammetry (DPV) in potentiostat Auto lab. 0.1M PBS as the electrolyte in electrochemical studies was prepared from 0.1M H_3PO_4 (99%, Sigma-Aldrich) and 0.1M NaH_2PO_4 (99%, Sigma-Aldrich). Scanning electron microscopy (SEM SU-8000, Hitachi, Tokyo, Japan) and X-ray diffraction (XRD, D5005, Siemens AG, Munich, Germany) techniques were used for characterization of the structure of the modified electrodes.

3. RESULT AND DISCUSSION

Figure 1 presents SEM images of as-deposited GQDs/GCE and Au-Ag NPs/GQDs/GCE. The SEM image of GQDs from Figure 1a shows large grains were electrodeposited on the surface of GCE with approximates the shape of a sphere. Moreover, aggregation and agglomeration of GQDs particles cause to form larger clusters. The average diameter of GQDs particles is ~ 100 nm. SEM images of Au NPs/GQDs/GCE, Ag NPs/GQDs/GCE and Au-Ag NPs/GQDs/GCE from Figures 1b to 1d display a uniform coverage of the metallic nanoparticles with smaller size on the GQDs surface which illustrated to own the more electroactive and absorption sites and it caused to enhance the interaction area and charge transfer rate on the surface of the modified electrodes. The average diameters of Au NPs, Ag NPs, and Au-Ag NPs are ~ 50 , 45, and 40nm, respectively.

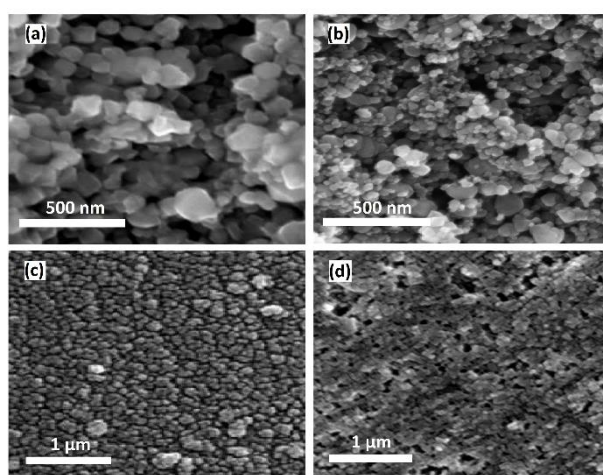


Figure 1. SEM images of as deposited (a) GQDs/GCE, (b) Au NPs/GQDs/GCE, (c) Ag NPs/GQDs/GCE and (d) Au-Ag NPs/GQDs/GCE.

Results of XRD analyses of powder of electrodeposited films are shown in Figure 2. For the GQDs, XRD pattern in Figure 2a shows the sharp diffraction peak at 26.67° which assigned to of graphitic (002) basal plane (JCPDS card No 75-207). The XRD pattern of Ag NPs/GQDs sample in Figure 2b shows the strong diffraction peaks at 38.12° , 44.29° , 64.56° and 77.49° which corresponds to the formation of the face-centered cubic (fcc) Ag nanoparticles with (111), (200), (220) and (311) crystallographic planes [26, 27] (JCPDS card No 04-0784). As observed from Figure 2c, the XRD pattern of Au NPs/GQDs sample depicts the diffraction peaks at 38.13° , 44.35° , 64.59° and 77.59° which can be well indexed to (111), (200), (220), (311) and (222) planes of fcc phase of Au crystal [28] (JCPDS card No 04-0783). The XRD pattern of the bimetallic alloy of Au-Ag shows the same characteristic peaks (111), (200), (220), (311), and (222) that it confirmed to formation of fcc structure of Au-Ag alloy on GQDs [29, 30]. Moreover, the presence of the peak (002) GQDs in all XRD patterns of metallic nanoparticles are evidence to electrodeposition of nanoparticles on GQDs and as well as indicated to maintain the crystalline structure with variation of the deposition materials [31, 32].

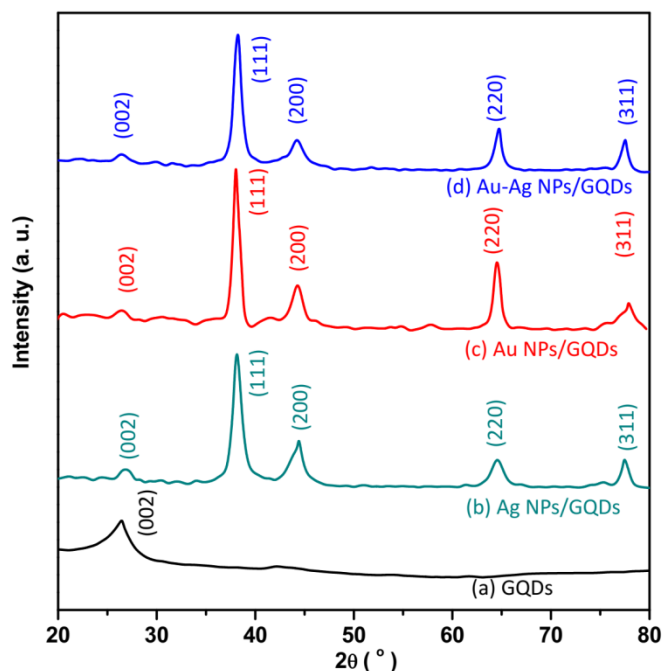


Figure 2. XRD patterns of powder of electrodeposited (a) GQDs, (b) Ag NPs/GQDs, (c) Au NPs/GQDs and (d) Au-Ag NPs/GQDs.

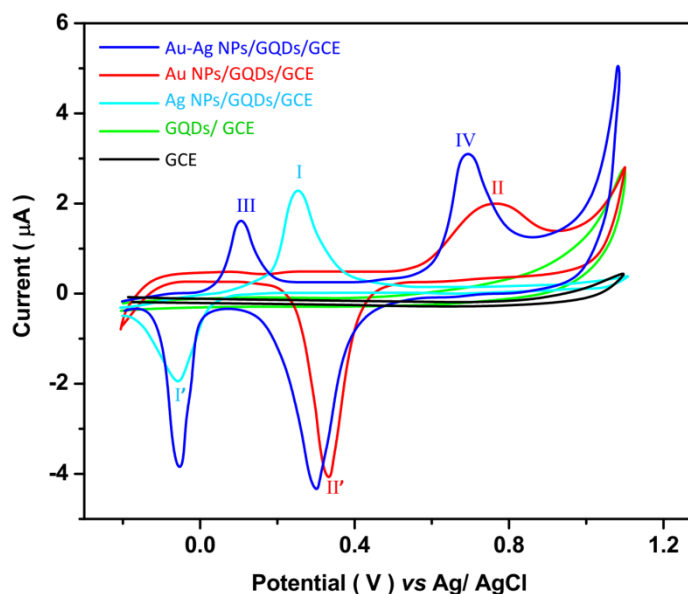


Figure 3. CV of GCE, GQDs/ GCE, Ag NPs/GQDs/GCE, Au NPs/GQDs/GCE and Au-Ag NPs/GQDs/GCE in 0.1M PBS and pH value of 7 at 10mV/s scan rate.

Figure 3 reveals the CV of GCE, GQDs/ GCE, Ag NPs/GQDs/GCE, Au NPs/GQDs/GCE and Au-Ag NPs/GQDs/GCE in 0.1M PBS and pH value of 7 at 10mV/s scan rate. The CV curves of GCE and GQDs/ GCE show only the background curves and no redox peaks observed for both of them. As seen from the CV of Ag NPs/GQDs/GCE, the anodic and cathodic peaks of Ag NPs are observed at 0.25 V (I) and -0.06 V (I') that relates to the oxidation of the Ag^0 into Ag^+ , and the reduction of Ag^+ to Ag^0 , respectively [33]. The CV of Au NPs/GQDs/GCE also showed the anodic and cathodic peaks at 0.77 V (II) and 0.33 V (II'), referring to oxidation and reduction of Au [34]. The CV curve of an Au-Ag NPs/GQDs/ GCE indicates both redox peaks of Ag and Au NPs at the surface of GQDs/ GCE. However, the oxidation peak of Ag and Au in the Au-Ag NPs alloy is observed at a lower positive potential of 0.10 V (III) and 0.68 V (IV), respectively toward the pure Ag NPs and Au NPs, demonstrating to the Au-Ag alloys are more active than pure silver nanoparticles due to combination of the advantages of Au NPs and Ag NPs simultaneously [35, 36]. In other words, Au-Ag NPs exhibits more favorable chemo-physical properties than their monometallic counterpart because of enhancement of local electric field in the alloy nanoparticles and the localization of highly dense strong hot spots and a large specific area on the porous Au-Ag NPs [37, 38]. Moreover, Au-Ag alloy can act as an electron transport channel to accelerate the charge transport [35].

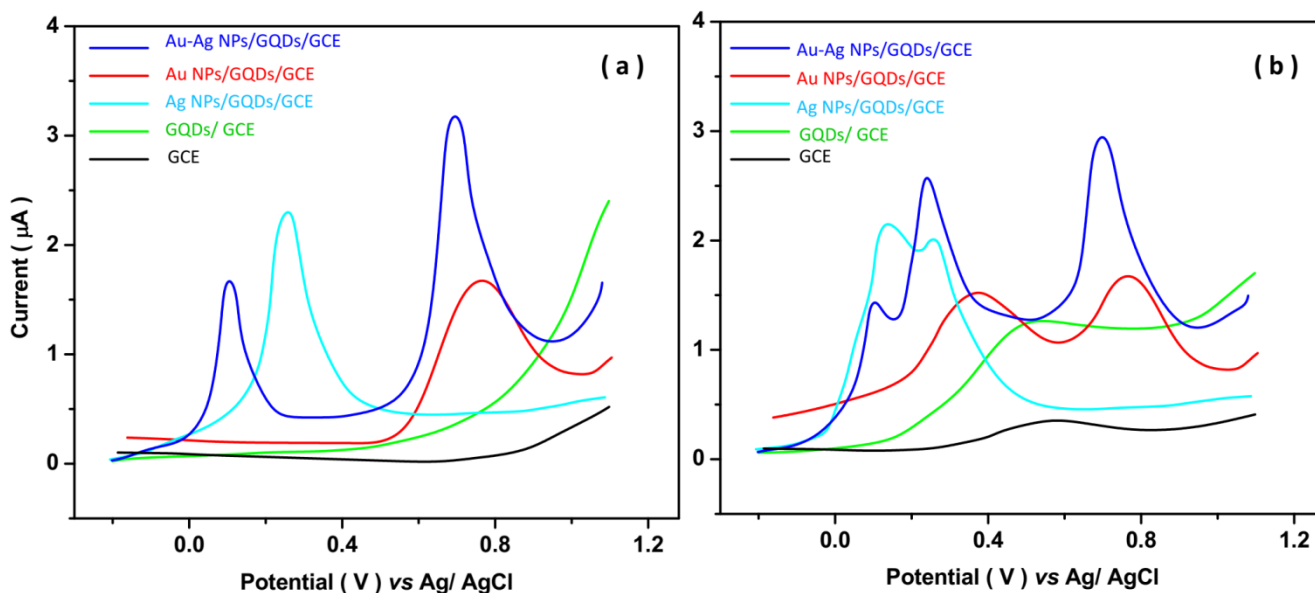
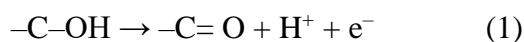


Figure 4. DPV of GCE, GQDs/ GCE, Ag NPs/GQDs/GCE, Au NPs/GQDs/GCE and Au-AgNPs/GQDs/GCE in 0.1M PBS and pH value of 7 at 10mV/s scan rate (a) before and (b) after addition of 10 μ M insulin solution.

Figure 4 shows the DPV curves of GCE, GQDs/ GCE, Ag NPs/GQDs/GCE, Au NPs/GQDs/GCE and Au-Ag NPs/GQDs/GCE in 0.1M PBS and pH value of 7 at 10mV/s scan rate before and after addition of 10 μ M insulin solution. Before the addition of insulin, there are not the significant peaks for DPV curves of GCE, GQDs/ GCE. The DPV of Ag NPs/GQDs/GCE, Au NPs/GQDs/GCE show the cathodic peaks at 0.25 V and 0.77 V that related to oxidation of Ag⁰ into Ag⁺ and Au⁰ into Au⁺, respectively. The DPV curve of Au-Ag NPs/GQDs/GCE shows the cathodic peaks of silver and gold at 0.10 V and 0.68 V, respectively. After the addition of insulin, the DPV curves of GCE, GQDs/ GCE, Ag NPs/GQDs/GCE, Au NPs/GQDs/GCE and Au-Ag NPs/GQDs/GCE display the oxidation peak of insulin at 0.57, 0.51, 0.36, 0.37 and 0.22 V, respectively that associated with electrochemical oxidation of redox-active hydroxyl groups of tyrosine residues on the insulin molecules according to electrochemical mechanism in equation (1) [39].



Comparison between the GCE and GQDs/ GCE reveals the GQDs effect on the enhancement of four times peak current of the electrode to the determination of insulin that attributed to GQDs film role on acceleration the electron transfer rate of insulin and excellent electrocatalytic activity for oxidation of insulin due to the high conductivity, owing to greater the affinity of electron movement with a steady reaction rate and inherent ability of GQDs [40, 41]. Furthermore, studies showed the units containing hydroxyl and carboxyl attached to the GQDs edges can enhance the surface functionality [42, 43]. Moreover, the oxidation peaks of Ag and Au NPs are also observed for Ag NPs/GQDs/GCE, Au NPs/GQDs/GCE and Au-Ag NPs/GQDs/GCE. In addition, the higher current and lower potential of oxidation peak of insulin on metallic nanoparticles is observed for Au-Ag

NPs/GQDs/GCE. Therefore, Au-Ag NPs/GQDs/GCE was selected for the following electrochemical studies for the determination of insulin.

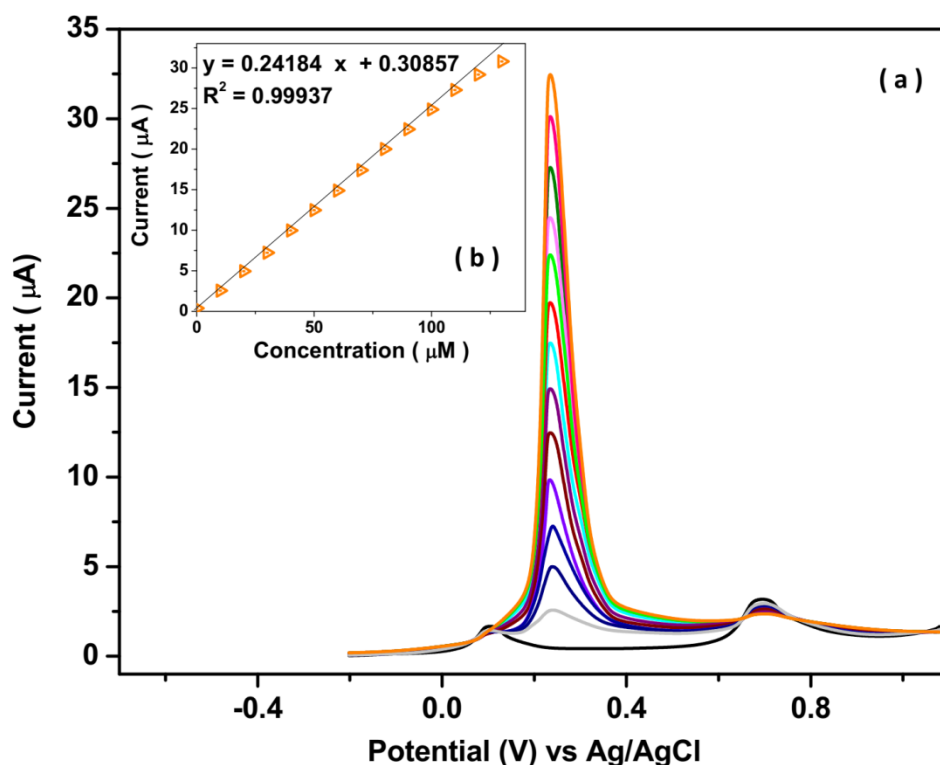


Figure 5. (a) DPV of Au-AgNPs/GQDs/GCE in 0.1M PBS and pH value of 7 at 10mV/s scan rate with successive addition of 10 μM insulin; (b) The calibration plot.

Figure 5a shows the study of concentration effect of insulin through the DPV responses of Au-Ag NPs/GQDs/GCE to successive addition of 10 μM insulin solutions in 0.1M PBS and pH value of 7 at 10mV/s scan rate. As seen, the oxidation peak of insulin at 0.22 V is linearly increased with increasing the insulin content in electrochemical cell, and the current of cathodic peaks of oxidation Ag and Au NPs at 0.10 V and 0.68 V do not change, respectively that it confirms the potential of 0.22 V is the oxidation potential of insulin on Au-Ag NPs/GQDs/GCE. The resulted calibration plot is shown in Figure 5b which indicated to a linear range of 10 to 120 μM, the limit of detection of 1.1 nM and sensitivity of 0.24184 μA/μM. These results are compared with sensing results of other reported insulin sensors in the literature in Table 1 that it evidence to the comparable or better linear range and detection limit of Au-Ag NPs/GQDs/GCE to electrochemical detection of insulin due to combination of high chemical stable Nobel nanostructured material with high redox-active mediated of silver nanoparticles on a porous substrate of GQDs which formed the high specific surface area and high electrical signal [43-46].

Table 1. Comparison between the sensing results of Au-Ag NPs/GQDs/GCE with the other reported insulin sensors in the literature.

Electrode	Limit of detection (nM)	Linear range (μM)	Ref.
CNTs/GCE	14	0.001-1	[47]
Ni doped carbon composite electrode	40	0.000015-0.001	[48]
MWNTs/dihydropyran/GCE	1000	0.8 – 2.5	[49]
Molecularly imprinted polymers/MWCNTs/pencil graphite electrode	0.0186	-	[50]
Red blood cells/Carbon paste electrode	6	0.006–0.09	[51]
Poly(pyropropionic acid)/MWCNTs/ GCE	0.2	0.5–1000	[52]
Ni(OH) ₂ /Nafion-MWCNTs	85	0.1–10	[53]
RuO ₂ /carbon fiber	23.0	0.10–1.00	[54]
Ni NPs/ITO	0.1	0.001–0.125	[55]
Co(OH) ₂ /carbon ceramic electrode	0.11	-	[56]
Silica gel	0.036	0.00009–0.0004	[57]
NiO-MWCNTs	6.1	0.020–0.26	[58]
Aptamer@Au-o-phenylenediamine/pencil graphite electrode	0.027	0.001–0.1	[59]
Au-AgNPs/GQDs/GCE	1.1	10-120	This work

The selectivity of the proposed insulin sensor was investigated in the presence of biological species human serum samples such as thiourea, glucose, methionine, cysteine, ascorbic acid, uric acid, and glutathione. Table 2 presents the results of study the interference effect on DPV response Au-Ag NPs/GQDs/GCE for the determination of 1 μM insulin at scan rate 10mV/s in successive additions of 10 μM of the biological species human serum. It is found that there are the negligible electrocatalytic currents to successive addition of foreign species at 0.22 V, and significant peak current is obtained to the addition of insulin, indicating the interference biological species in Table 2 do not show any interference effect on insulin determination and excellent selectivity of Au-Ag NPs/GQDs/GCE [60].

Table 2. Peak currents of DPV of Au-Ag NPs/GQDs/GCE at 0.22 V in 0.1M PBS and pH value of 7 at 10mV/s scan rate with successive addition of 1µM insulin and 10µM of the biological species human serum.

Species	Added (µM)	Peak current (µA)	RSD (%)
Insulin	1	0.2398	±0.0112
Thiourea	10	0.0110	±0.0048
Glucose	10	0.0081	±0.0017
Methionine	10	0.0098	±0.0011
C-peptide	10	0.0072	±0.0012
Cysteine	10	0.0020	±0.0010
Ascorbic acid	10	0.0102	±0.0022
Uric acid	10	0.0089	±0.0011
glutathione	10	0.0071	±0.0007

For study the applicability of the Au-Ag NPs/GQDs/GCE as insulin sensor in Lantus (insulin glargine injection) sample, the corresponding DPV curves of the prepared real sample of Lantus in 0.1M PBS and pH value of 7 at 10mV/s scan rate with successive addition of 10 mM insulin is shown in Figure 6a. Before the addition of insulin, DPV curves shows four peaks at 0.10, 0.67, 0.22, and 0.40 V which attributed the oxidation of Ag, Au on electrode surface and insulin and interference species in Lantus sample, respectively.

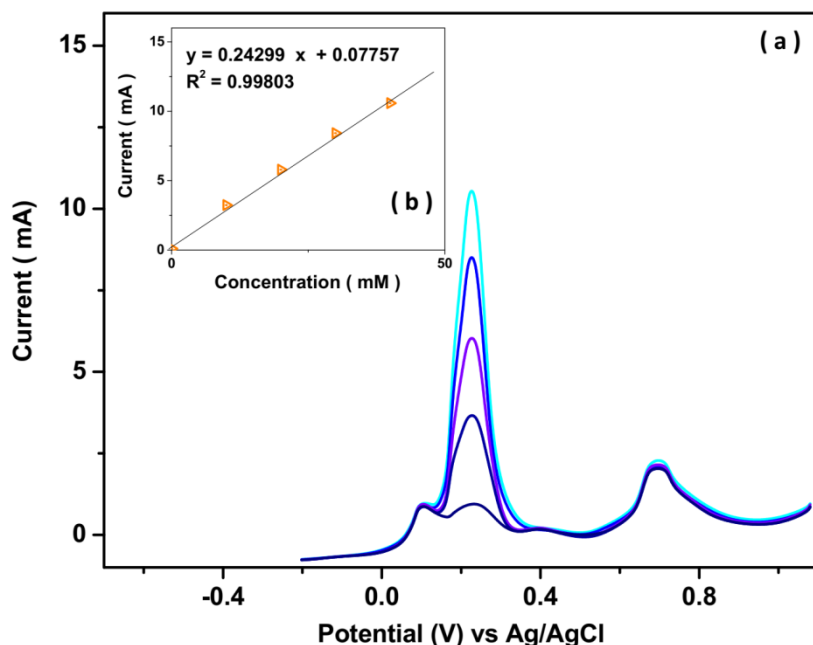


Figure 6. (a) DPV curves of prepared real sample of Lantus in 0.1M PBS and pH value of 7 at 10mV/s scan rate with successive addition of 10 mM insulin; (b) The calibration plot.

After successive addition of insulin, the anodic peak at 0.22 V is increased by increasing the insulin concentration in an electrochemical cell, and the peaks related to the oxidation of Au, Ag on the electrode surface and interference species in the Lantus sample are not changed. The obtained

calibration plot in Figure 6b shows that the insulin concentration in the initial Lantus sample is 0.636 mM which is in good agreement with the labeled value. Moreover, Table 3 displays the acceptable values for recovery (more than 96.3%) and relative standard derivation (RSD) (less than 4.53%), demonstrating the proposed sensor can be used as a reliable and precise sensor for the determination of insulin in biological and clinical samples.

Table 3. Analytical results of analysis insulin in the real sample of Lantus.

Sample	Added (mM)	Measured (mM)	Recovery (%)	RSD (%)
Lantus	10.0	9.8	98.0	3.02
	20.0	19.6	98.0	3.24
	30.0	28.9	96.3	4.53
	40.0	38.8	97.0	4.01

4. CONCLUSION

This study presented the synthesis of Au-Ag NPs/GQDs/GCE and application as a highly sensitive electrochemical sensor of insulin level in prescription drugs for type 2 diabetic patients. To synthesize the modified electrode, GQDs were synthesized using the hydrothermal method and electrodeposited on GCE, and then Au-Ag NPs were electrodeposited on GQDs/GCE. The results of structural analyses showed uniform coverage of the bimetallic nanoparticles in fcc crystal structure on the GQDs. The electrochemical studies showed that the linear range, limit of detection and sensitivity were obtained 10 to 120 μ M, 1.1nM and 0.24184 μ A/ μ M, respectively which were comparable or better than sensing results of other reported insulin sensors in the literature. Results of the study the selectivity of the proposed insulin sensor showed that thiourea, glucose, methionine, cysteine, ascorbic acid, uric acid and glutathione did not show any interference effect on insulin determination. The applicability of sensor was studied to determination of insulin in insulin glargine injection sample and results exhibited to the acceptable values for recovery and RSD, indicating the proposed sensor can be used as a reliable and precise sensor for the determination insulin in biological and clinical samples.

References

1. J. Lu, C. Wang, Y. Shen, L. Chen, L. Zhang, J. Cai, W. Lu, W. Zhu, G. Hu and T. Xia, *Diabetes Care*, 44 (2021) 549.
2. S. Yang, Z. Li, K. Yan, X. Zhang, Z. Xu, W. Liu, Z. Liu and H. Liu, *Journal of Environmental Sciences*, 103 (2021) 59.
3. H. Mather, J.A. Nisbet, G. Burton, G. Poston, J. Bland, P.A. Bailey and T. Pilkington, *Clinica Chimica Acta*, 95 (1979) 235.
4. O.E. Kale, M. Vongdip, T.F. Ogundare and O. Osilesi, *Toxicology Mechanisms and Methods*, 45 (2020) 1.

5. J.L. González-Solís, J.R. Villafan-Bernal, B. Martínez-Zérega and S. Sánchez-Enríquez, *Lasers in medical science*, 33 (2018) 1791.
6. Z. Dai, J. Xie, Z. Chen, S. Zhou, J. Liu, W. Liu, Z. Xi and X. Ren, *Chemical Engineering Journal*, 410 (2021) 128341.
7. M. Zhang, L. Zhang, S. Tian, X. Zhang, J. Guo, X. Guan and P. Xu, *Chemosphere*, 253 (2020) 126638.
8. C.G. Awuchi, C.K. Echeta and V.S. Igwe, *Health Sciences Research*, 6 (2020) 5.
9. Z. Dai, S. Guo, Y. Gong and Z. Wang, *Ceramics International*, 47 (2021) 6535.
10. Y. Yang, H. Chen, X. Zou, X.-L. Shi, W.-D. Liu, L. Feng, G. Suo, X. Hou, X. Ye and L. Zhang, *ACS applied materials & interfaces*, 12 (2020) 24845.
11. H. Zhao, X. Liu, L. Yu, S. Lin, C. Zhang, H. Xu, Z. Leng, W. Huang, J. Lei and T. Li, *Molecular Therapy-Nucleic Acids*, 23 (2021) 667.
12. Y. Shen, W. Prinyawiwatkul and Z. Xu, *Analytst*, 144 (2019) 4139.
13. W. Jiang, L. Gao, P. Li, H. Kan, J. Qu, L. Men, Z. Liu and Z. Liu, *Journal of Chromatography B*, 1044 (2017) 8.
14. X. Li, T. Shi, B. Li, X. Chen, C. Zhang, Z. Guo and Q. Zhang, *Materials & Design*, 183 (2019) 108152.
15. M. Sk, S. Banesh, V. Trivedi and S. Biswas, *Inorganic chemistry*, 57 (2018) 14574.
16. Y. Sun, Y. Lin, W. Sun, R. Han, C. Luo, X. Wang and Q. Wei, *Analytica chimica acta*, 1089 (2019) 152.
17. Z. Dai, J. Xie, X. Fan, X. Ding, W. Liu, S. Zhou and X. Ren, *Chemical Engineering Journal*, 397 (2020) 125520.
18. F. Kartal, D. Çimen, N. Bereli and A. Denizli, *Materials Science and Engineering: C*, 97 (2019) 730.
19. J. Hovancová, I. Šišoláková, R. Oriňaková and A. Oriňak, *Journal of Solid State Electrochemistry*, 21 (2017) 2147.
20. L. Ding and H. Zhang, *International Journal of Electrochemical Science*, 12 (2017) 11163.
21. K. Zhang, Z. Cao, S. Wang, J. Chen, Y. Wei and D. Feng, *International Journal of Electrochemical Science*, 15 (2020) 2604.
22. F. Faridbod, M.R. Ganjali, E. Nasli-Esfahani, B. Larijani, S. Riahi and P. Norouzi, *International Journal of Electrochemical Science*, 5 (2010) 880.
23. C. Wang, J. Qian, K. Wang, M. Hua, Q. Liu, N. Hao, T. You and X. Huang, *ACS applied materials & interfaces*, 7 (2015) 26865.
24. Y. Yu, W. Liu, J. Ma, Y. Tao, Y. Qin and Y. Kong, *RSC advances*, 6 (2016) 84127.
25. J. Tang, R. Huang, S. Zheng, S. Jiang, H. Yu, Z. Li and J. Wang, *Microchemical Journal*, 145 (2019) 899.
26. S. Bykkam, M. Ahmadipour, S. Narisngam, V.R. Kalagadda and S.C. Chidurala, *Advances in Nanoparticles* 4(2015) 1.
27. X. Wang, Z. Feng, B. Xiao, J. Zhao, H. Ma, Y. Tian, H. Pang and L. Tan, *Green Chemistry*, 22 (2020) 6157.
28. M.R. Shaik, S.F. Adil, M. Kuniyil, M. Sharif, A. Alwarthan, M.R.H. Siddiqui, M. Ali, M.N. Tahir and M. Khan, *Applied Sciences*, 10 (2020) 503.
29. S. Yallappa, J. Manjanna and B. Dhananjaya, *Spectrochimica Acta Part A: Molecular and Biomolecular Spectroscopy*, 137 (2015) 236.
30. Y. Zhang, G. Gao, Q. Qian and D. Cui, *Nanoscale research letters*, 7 (2012) 1.
31. Z. Chen, H. Zhang, X. He, G. Fan, X. Li, Z. He, G. Wang and L. Zhang, *BioResources*, 16 (2021) 2644.
32. H. Karimi-Maleh, Y. Orooji, F. Karimi, M. Alizadeh, M. Baghayeri, J. Rouhi, S. Tajik, H. Beitollahi, S. Agarwal and V.K. Gupta, *Biosensors and Bioelectronics*, 184 (2021) 113252.

33. S.N. Mailu, T.T. Waryo, P.M. Ndagili, F.R. Ngece, A.A. Baleg, P.G. Baker and E.I. Iwuoha, *Sensors*, 10 (2010) 9449.
34. J. Lović, S. Stevanović, N.D. Nikolić, S. Petrović, D. Vuković, N. Prlainović, D. Mijin and M.A. Ivić, *International Journal of Electrochemical Science*, 12 (2017) 5806.
35. M. Hasanzadeh and N. Shadjou, *Microchimica Acta*, 184 (2017) 389.
36. L. Zhang, J. Zheng, S. Tian, H. Zhang, X. Guan, S. Zhu, X. Zhang, Y. Bai, P. Xu and J. Zhang, *Journal of Environmental Sciences*, 91 (2020) 212.
37. C. Awada, C. Dab, M. Grimaldi, A. Alshoaibi and F. Ruffino, *Scientific reports*, 11 (2021) 1.
38. H. Karimi-Maleh, M.L. Yola, N. Atar, Y. Orooji, F. Karimi, P.S. Kumar, J. Rouhi and M. Baghayeri, *Journal of colloid and interface science*, 592 (2021) 174.
39. A. Noorbakhsh and A.I.K. Alnajjar, *Microchemical Journal*, 129 (2016) 310.
40. N. Hashemzadeh, M. Hasanzadeh, N. Shadjou, J. Eivazi-Ziaei, M. Khoubnasabjafari and A. Jouyban, *Journal of Pharmaceutical Analysis*, 6 (2016) 235.
41. H. Karimi-Maleh, S. Ranjbari, B. Tanhaei, A. Ayati, Y. Orooji, M. Alizadeh, F. Karimi, S. Salmanpour, J. Rouhi and M. Sillanpää, *Environmental Research*, 195 (2021) 110809.
42. S. Sarabiyan Nejad, A. Babaie, M. Bagheri, M. Rezaei, F. Abbasi and A. Shomali, *Polymers for Advanced Technologies*, 31 (2020) 2279.
43. B.A. Al Jahdaly, M.F. Elsadek, B.M. Ahmed, M.F. Farahat, M.M. Taher and A.M. Khalil, *Sustainability*, 13 (2021) 2127.
44. H. Katas, N.Z. Moden, C.S. Lim, T. Celesistinus, J.Y. Chan, P. Ganasan and S. Suleman Ismail Abdalla, *Journal of Nanotechnology*, 2018 (2018) 1.
45. M. A Bhosale and B. M Bhanage, *Current Organic Chemistry*, 19 (2015) 708.
46. P. Tian, L. Tang, K. Teng and S. Lau, *Materials today chemistry*, 10 (2018) 221.
47. J. Wang and M. Musameh, *Analytica Chimica Acta*, 511 (2004) 33.
48. A. Salimi, M. Roushani, S. Soltanian and R. Hallaj, *Analytical Chemistry*, 79 (2007) 7431.
49. R.M. Snider, M. Ciobanu, A.E. Rue and D.E. Cliffler, *Analytica Chimica Acta*, 609 (2008) 44.
50. B.B. Prasad, R. Madhuri, M.P. Tiwari and P.S. Sharma, *Electrochimica Acta*, 55 (2010) 9146.
51. A. Kaur and N. Verma, *European Journal of Experimental Biology*, 2 (2012) 389.
52. V. Serafín, L. Agüí, P. Yáñez-Sedeño and J. Pingarrón, *Biosensors and Bioelectronics*, 52 (2014) 98.
53. E. Martínez-Periñán, M. Revenga-Parra, M. Gennari, F. Pariente, R. Mas-Ballesté, F. Zamora and E. Lorenzo, *Sensors and Actuators B: Chemical*, 222 (2016) 331.
54. W. Gorski, C.A. Aspinwall, J.R. Lakey and R.T. Kennedy, *Journal of Electroanalytical Chemistry*, 425 (1997) 191.
55. Y. Yu, M. Guo, M. Yuan, W. Liu and J. Hu, *Biosensors and Bioelectronics*, 77 (2016) 215.
56. E. Habibi, E. Omidinia, H. Heidari and M. Fazli, *Analytical biochemistry*, 495 (2016) 37.
57. M. Jaafariasl, E. Shams and M.K. Amini, *Electrochimica Acta*, 56 (2011) 4390.
58. B. Rafiee and A.R. Fakhari, *Biosens Bioelectron*, 46 (2013) 130.
59. A.A. Ensafi, E. Khoddami and B. Rezaei, *Colloids and Surfaces B: Biointerfaces*, 159 (2017) 47.
60. H. Karimi-Maleh, M. Alizadeh, Y. Orooji, F. Karimi, M. Baghayeri, J. Rouhi, S. Tajik, H. Beitollahi, S. Agarwal and V.K. Gupta, *Industrial & Engineering Chemistry Research*, 60 (2021) 816.